

A UNIQUE SUPERNOVA GRAPHITE: CONTEMPORANEOUS CONDENSATION OF ALL THINGS CARBONACEOUS. T. K. Croat, M. Jadhav, E. Lebsack and T. J. Bernatowicz, Laboratory for Space Sciences and Department of Physics, Washington University, St. Louis, MO 63130, USA, tkc@wustl.edu.

Introduction: Correlated TEM and SIMS investigations of presolar graphites have shown that graphite is very effective at capturing and preserving internal grains of other more refractory phases during its growth, with a single graphite often containing hundreds of internal grains [1]. From isotopic and TEM measurements of such grain assemblages, one can reconstruct a grain's formation history, which can provide important tests of supernova (SN) nucleosynthesis and grain condensation processes. Here we present TEM results from an Orgueil SN graphite that contains internal TiCs with various epitaxial refractory phases, including kamacite, nickel silicide (Ni_2Si) and SiC. Internal grains of SiC and kamacite/iron silicide are also found independent of TiC. The grain microstructures suggest primary formation of each of these phases directly from the gas, in some cases heterogeneously nucleating on existing solid surfaces of the more refractory TiCs. This single graphite contains all of the phases that equilibrium thermodynamic calculations predict will form in C-rich SN layers [2], confirming to some degree the applicability of such calculations even to complex SN environments.

Experimental Methods: Graphite OR1d3m-18 (7 μm diameter) from the OR1d density and size separate (1.75-1.92 g cm^{-3} , $>1 \mu\text{m}$) of the Orgueil meteorite [3] was identified as a SN graphite based on NanoSIMS C, O, N and Si isotopic measurements. This graphite was picked from the mount, embedded in resin, and then sliced into $\sim 70 \text{ nm}$ ultramicrotome sections, 11 of which were suitable for TEM study. The slices were retrieved on holey carbon-coated copper TEM grids and examined in a JEOL 2000FX analytical TEM equipped with a NORAN Energy Dispersive X-ray Spectrometer (EDXS).

Results: Graphite g18 (Fig. 1a) shows ^{12}C , ^{15}N , ^{18}O and ^{28}Si enrichments that are characteristic of grains originating in a SN (isotopic ratios of $^{12}\text{C}/^{13}\text{C} = 75.9 \pm 0.4$, $^{14}\text{N}/^{15}\text{N} = 230 \pm 14$, $^{16}\text{O}/^{18}\text{O} = 286 \pm 5$, $\delta^{29}\text{Si} = -89 \pm 9$, and $\delta^{30}\text{Si} = -102 \pm 11$). Many internal titanium carbides (TiCs) were found, with $\sim 60 \text{ nm}$ average diameter and constituting $\sim 300 \text{ ppm}$ by volume. V and Si were also present in the TiCs (avg. atomic ratios of $\text{V}/\text{Ti} \sim 0.08$ and $\text{Si}/\text{Ti} \sim 0.40$). No evidence of s-process element enrichments were found (Zr, Mo not detected), which is consistent with results for previous SN carbides [1]. The abnormally high Si content, exceeding that which is normally found in solid solution, can be explained by the presence of SiC layers grown

onto the TiC surfaces. Figures 1b and 1c show image and diffraction data from such a TiC/SiC grain and Fig. 1d is a dark-field image formed from one of the SiC diffraction spots in Fig. 1c, with the bright surface coating indicating the SiC's location. This identification is confirmed with EDXS, wherein the SiC edge region shows a 2x higher Si/Ti ratio than the TiC center. Such a SiC coating on TiC was evident on nearly every TiC (111) face that was examined. Other refractory carbides had large distinct SiC regions of comparable size to the TiC (Fig. 1e). The inset dark-field (DF) image formed from a SiC diffracted spot shows a SiC domain with several stacking faults that comprises

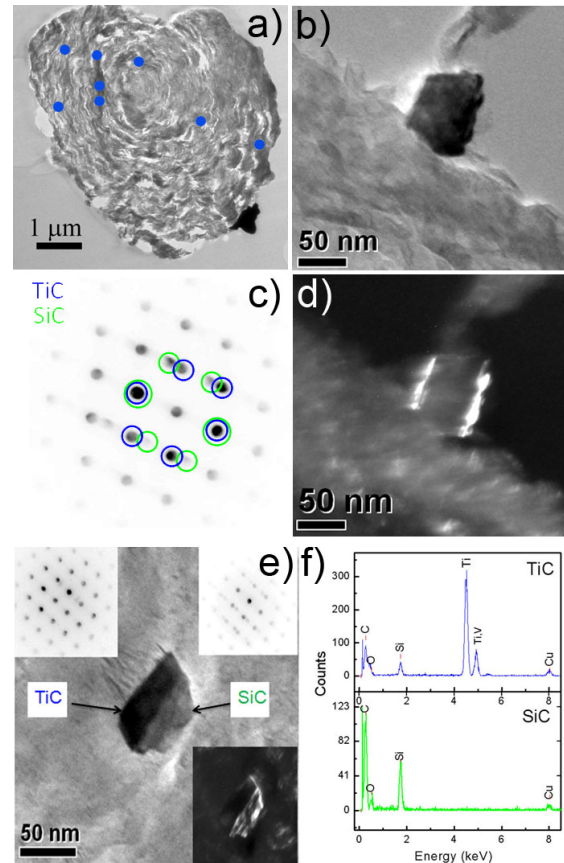


Fig. 1. a) Bright-field (BF) image of g18 graphite with internal TiCs indicated by blue dots b) bright-field image of TiC and c) microdiffraction pattern taken from edge of 1b showing SiC coating phase grown onto TiC face. d) DF image from SiC spot revealing SiC coatings (bright) on opposite (111) TiC faces e) BF and DF images of TiC/SiC composite grain including diffraction patterns and f) EDXS from each side.

about half of the carbide. EDXS (Fig. 1f) of both regions in Fig. 1e show very low Ti content in the SiC region, but still significant Si in the TiC possibly due to SiC coatings surrounding other TiC faces. Three SiCs were also found independent of TiC.

This graphite also contains 3 TiCs with attached Ni,Si-rich grains and one with attached Fe,Si-rich grains. Electron diffraction patterns of three of the larger Ni,Si-rich grains (40-50 nm in diameter) are all consistent with the known Ni₂Si phase (orthorhombic; $a = 7.10\text{\AA}$, $b = 5.15\text{\AA}$, $c = 4.08\text{\AA}$), and numerous high-symmetry zones were indexed, including [111], [112] and [110] zones. Fig. 2a shows a TiC with an attached Ni₂Si grain and microdiffraction patterns from each which show alignment of low index zones from each phase. Another instance of a TiC/Ni₂Si composite grain was found with separate Ni₂Si grains on opposite faces of the same TiC. Both microstructures indicate epitaxial growth of nickel silicide on existing TiC grains. EDXS of three Ni₂Si grains all agree with the known phase stoichiometry, showing (Ni_{1-x}Fe_x)₂Si with $0.05 < x < 0.1$.

A TiC was found with Fe,Si-rich grains attached to two separate faces (Fig 2b). The [011] TiC zone was found parallel to [001] kamacite zones (2.9Å BCC) in both kamacites. The Fe,Si-rich grains have compositions of Fe₆₄Ni₁₄Si₂₁ and Fe₆₈Ni₉Si₂₃, which is an abnormally high Si content for metallic iron. Weak spots in the kamacite [001] diffraction patterns, near the forbidden (100) BCC kamacite spot, suggest presence of a second iron silicide phase in solid solution with kamacite. Another FeSi-rich grain is found independent of TiC (Fig. 2c) and consists of three separate crystalline domains all with a composition near Fe₆₇Ni₇Si₂₇. Diffraction patterns taken from the lower domain are consistent with [001] and [112] kamacite, but contain additional weak spots at a 3.29Å spacing. These spots in the [112] zone are consistent with {111} planes of Fe₂Si (cubic, 5.7Å, Pearson CF16). The extra forbidden diffraction spots in the Fig. 2b pattern are also consistent with cubic Fe₂Si. A solitary 30 nm grain of composition Fe₅₈Ni₁Si₃₄Al₅ was also found, with a diffraction pattern consistent with [011] kamacite, but in this case no indications of the cubic Fe₂Si phase.

Discussion: Many features seen in g18 have been discovered previously in other SN graphites [1, 4], but g18 is unique in that it contains all of the phases predicted to form in C-rich SN zones [2]. Observed microstructural features (e.g. separate Ni₂Si grains heterogeneously nucleated and grown onto different faces of a single TiC) demonstrate a phase condensation sequence of TiC, followed by Ni₂Si, Si-rich kamacite/Fe₂Si, SiC (with relative order undetermined) and finally graphite. This is roughly consistent with predictions [2], although at the high C/O ratios of undiluted

C-rich SN zones, graphite would condense first rather than last. Iron and nickel silicides have also been reported within SiC-X grains [5], but in that case appear to form secondarily at grain boundaries between SiC domains rather than being direct condensates from the gas. Presence of Fe-Ni silicides, SiC, and Si-rich kamacite within graphite all suggest higher Si content in the SN environment from which g18 condensed, possibly due to a greater contribution from the Si/S zone (which is also consistent with the ²⁸Si enrichment).

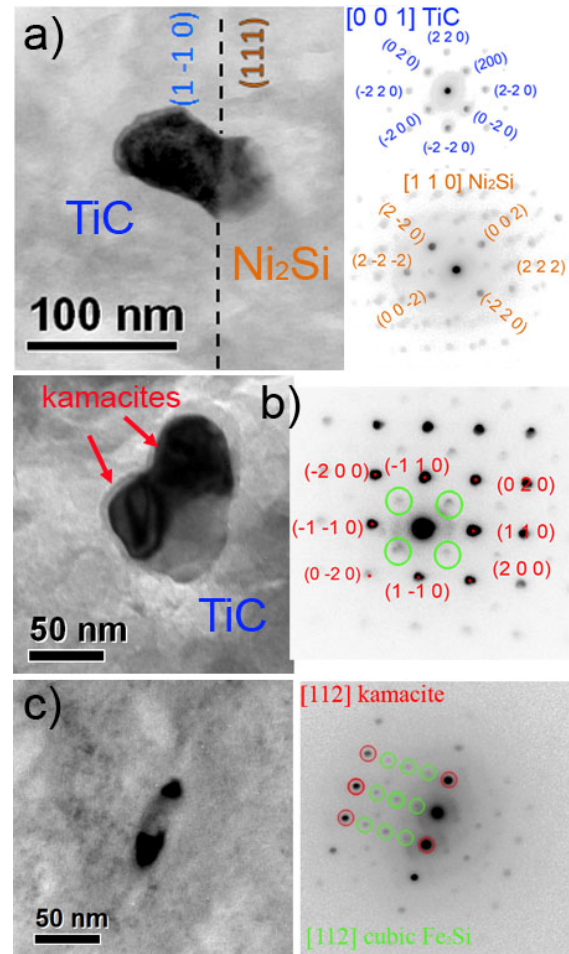


Fig.2. a) BF image and microdiffraction patterns of TiC with Ni₂Si attached to its (1 -1 0) face. b) BF image of TiC with 2 attached kamacites and diffraction pattern from upper kamacite with extra Fe₂Si spots c) BF image of FeSi-rich phase consisting of 3 crystalline domains and diffraction pattern from lower domain.

Acknowledgments: We thank S. Amari and T. Maruoka for preparation of the Orgueil samples.

References: [1] Croat T.K. et al. (2003) *GCA*, 67, 4705. [2] Fedkin A.V. et al. (2010) *GCA*, 74, 3642. [3] Jadhav M. et al. (2006) *New Astron. Rev.* 50, 591. [4] Croat T.K. et al. (2009) *LPS XL*, Abstract # 2175. [5] Hynes et al. (2010) *MAPS* 45, 596.